Published in final edited form as:
Clin Cancer Res. 2014 November 1; 20(21): 5537–5546. doi:10.1158/1078-0432.CCR-13-3003.

Molecular Profiling of Patient-Matched Brain and Extracranial Melanoma Metastases Implicates the PI3K Pathway as a Therapeutic Target

Guo Chen[1], **Nitin Chakravarti**[2], **Kimberly Aardalen**[3], **Alexander J. Lazar**[2], **Michael T. Tetzlaff**[2], **Bradley Wubbenhorst**[4], **Sang-Bae Kim**[5], **Scott Kopetz**[6], **Alicia A. Ledoux**[2], **Y.N. Vashisht Gopal**[1], **Cristiano Goncalves Pereira**[1], **Wanleng Deng**[1], **Ju-Seog Lee**[5], **Katherine L. Nathanson**[4], **Kenneth D. Aldape**[2], **Victor G. Prieto**[2], **Darrin Stuart**[3], and **Michael A. Davies**[1]

[1]Department of Melanoma Medical Oncology, The University of Texas MD Anderson Cancer Center, Houston, TX 77030, USA

[2]Department of Pathology, The University of Texas MD Anderson Cancer Center, Houston, TX 77030, USA

[3]Novartis Institutes for Biomedical Research, Emeryville, CA 94608, USA

[4]Division of Medical Genetics, Department of Medicine, The University of Pennsylvania School of Medicine, Philadelphia, PA 19104, USA

[5]Department of Systems Biology, The University of Texas MD Anderson Cancer Center, Houston, TX 77030, USA

[6]Department of Gastrointestinal Medical Oncology, The University of Texas MD Anderson Cancer Center, Houston, TX 77030, USA

Abstract

Purpose—An improved understanding of the molecular pathogenesis of brain metastases, one of the most common and devastating complications of advanced melanoma, may identify and prioritize rational therapeutic approaches for this disease. In particular, the identification of molecular differences between brain and extracranial metastases would support the need for the development of organ-specific therapeutic approaches.

Experimental Design—Hotspot mutations, copy number variations (CNV), global mRNA expression patterns, and quantitative analysis of protein expression and activation by reverse phase protein array (RPPA) analysis were evaluated in pairs of melanoma brain metastases and extracranial metastases from patients who had undergone surgical resection for both types of tumors.

Corresponding author: Guo Chen, Department of Melanoma Medical Oncology, The University of Texas MD Anderson Cancer Center, Unit 0904, 1515 Holcombe Blvd, Houston, TX 77030; Phone: 713-792-8603; Fax: 713-563-3424; gchen2@mdanderson.org..

[1]http://www.mdanderson.org/education-and-research/resources-for-professionals/scientific-resources/core-facilities-and-services/functional-proteomics-rppa-core/index.html

Results—The status of 154 previously reported hotspot mutations, including driver mutations in *BRAF* and *NRAS,* were concordant in all evaluable patient-matched pairs of tumors. Overall patterns of CNV, mRNA expression, and protein expression were largely similar between the paired samples for individual patients. However, brain metastases demonstrated increased expression of several activation-specific protein markers in the PI3K/AKT pathway compared to the extracranial metastases.

Conclusions—These results add to the understanding of the molecular characteristics of melanoma brain metastases and support the rationale for additional testing of the PI3K/AKT pathway as a therapeutic target in these highly aggressive tumors.

Keywords

melanoma brain metastasis; molecular profiling; PI3K pathway; patient-matched samples; xenograft model

Introduction

Melanoma is the most aggressive form of skin cancer. In contrast to most other tumor types, the annual incidence of melanoma continues to rise, suggesting that it will be an increasingly important public health issue in the future (1, 2). One of the most common and devastating complications of melanoma is the development of metastases to the central nervous system (CNS). Lung cancer, breast cancer, and melanoma are the three most common sources of brain metastases (3). As melanoma is much less prevalent than lung or breast cancer, this reflects the heightened propensity of melanoma to metastasize to the brain-the highest among common malignancies. Up to 75% of stage IV melanoma patients will develop brain metastasis(es) during the course of their disease (4). The brain is often the first, and sometimes the only, site of disease progression in patients treated with systemic therapies (5). While multiple therapeutic modalities are used in patients with brain metastases, the median survival for these patients is ~4 months from diagnosis, and >50% of melanoma-related deaths are caused by brain metastases (6-10). Ipilimumab and dabrafenib are two new therapies approved by the US Food and Drug Administration for treating metastatic melanoma, but they showed only modest activities in patients with brain metastases, with median progression-free survivals (PFS) reported to be 1.4 and ~4 months, respectively(11, 12).

The treatment of patients with metastatic melanoma is evolving rapidly due to an improved understanding of the molecular underpinnings and heterogeneity of this disease. While there is a critical need for more effective treatments for melanoma patients with brain metastases, at this time there is very little information available about the molecular characteristics of these tumors. Broad molecular profiling studies in other tumors, such as breast cancer, have shown that tumors that metastasize to the brain can have distinct molecular features from tumors that metastasize to other sites (13). Other studies have demonstrated that brain metastases and extracranial metastases within individual patients can show marked molecular differences, including those in targetable pathways (e.g., EGFR in lung cancer (14-16)). In melanoma, previous studies examining individual proteins (e.g., P-STAT3, SOCS1) or pathways (e.g., PI3K/AKT) have identified significant differences in their

expression in brain and extracranial metastases, albeit in specimens from different patients (17-19). More recently, an immunohistochemical study of nine patients for MAPK and PI3K/AKT pathway activation markers demonstrated that P-AKT expression can be higher in brain metastases compared to extracranial metastases from the same patient (20). A broader transcriptional analysis of patient-matched brain and extracranial melanoma metastases also recently identified genes with differential levels of expression between brain and extracranial metastases, although this analysis failed to identify any significantly enriched pathways (21).

Together these previous studies support the rationale for broader profiling of brain metastases in order to improve our understanding of the molecular features of these tumors and to support development of rational therapeutic approaches. Here we report the results of high-throughput molecular analyses of matched pairs of melanoma brain and extracranial metastases from patients who underwent surgery for both types of tumors over the course of their disease as part of their standard clinical care. The assessable tissues were analyzed for known recurrent DNA hotspot mutations, DNA copy number variations (CNV), whole genome mRNA expression patterns, and the activation and expression of protein signaling networks. Analysis of the results from these different platforms supports that while patient-matched brain and extracranial metastases overall are quite similar, significant differences are observed in targetable pathways in brain metastases. In particular, our broad molecular analysis and early functional studies add to previous data supporting a critical role for activation of the PI3K/AKT pathway in these tumors.

Materials and Methods

Clinical Samples

Under a protocol approved by the Institutional Review Board of The University of Texas MD Anderson Cancer Center, tumors resected from melanoma patients between 1992 and 2010 were obtained from the MD Anderson Cancer Center Central Nervous System Tissue Bank and the Melanoma Informatics, Tissue Resource, and Procurement Core facility (MelCore). Samples were either formalin-fixed and paraffin-embedded (FFPE) tissue blocks (stored at room temperature) or optimal cutting temperature (OCT)-embedded frozen blocks (stored at −80°C) (Supplementary Table S1 and S2). CNV and gene expression data from these samples are available at Gene Expression Omnibus (GEO) database (accession number GSE50496).

Sample Processing

For each tumor sample used for analyte (DNA, RNA or protein) extraction, a hematoxylin and eosin (H&E)-stained slide was prepared and reviewed by a pathologist (AJL, KA). Regions containing 70% or more viable tumor cells were identified. To isolate tumor tissue, the marked H&E slide was used to guide macrodissection of the matched tissue block. Extraction of DNA (QIAamp DNA FFPE Tissue kit, Qiagen), RNA (22), and protein (23) from the dissected tumor samples was performed as previously described.

Mutation Detection

Genomic DNA samples extracted from FFPE tissues were genotyped using Sequenom mass array for the presence of any of more than 154 previously reported somatic hotspot mutations (Supplementary Table S3) by the MD Anderson Characterized Cell Line Core facility as previously described (24).

Copy Number Determination

Molecular inversion probes arrays (Affymetrix) (25) were used to identify genome-wide CNV in DNA extracted from FFPE tumor samples. DNA from normal tissues of the same patients was used as controls. Quality scores were calculated for each sample and samples with poor data quality were removed from further analysis. CNVs were then segmented using the SNP (single nucleotide polymorphism)-FASST2 (Fast Adaptive States Segmentation Technique) algorithm in Nexus 7.0 (Biodiscovery). For segmentation, the threshold (log2 scale) for a single copy gain/loss was set at +/− 0.3, and a high copy gain or a homozygous loss at +/− 1.2. Two-tailed Fisher's exact test was used to compare CNV frequency between brain and extracranial metastases.

Gene Expression Profiling

Total RNA was extracted from frozen tumors and subjected to whole-genome gene expression profiling using HumanHT12 v4 beadchip arrays (Illumina). RNA amplification (TotalPrep RNA Amplification Kit, Life Technologies), array hybridization, and data acquisition were performed at the University of Texas Health Science Center at Houston Microarray Core laboratory. Gene expression data were quantile-normalized and analyzed using BRB-ArrayTools (26). *P*-values for gene expression differences between brain and extracranial metastases were determined using a random variance model (27).

Reverse Phase Protein Array

Protein lysates extracted from frozen tumors were analyzed by RPPA at the MD Anderson Functional Proteomics Core facility as previously described (22). A detailed description of the RPPA method and data normalization is available at the core facility's web page[1] and antibodies used for RPPA are listed in Supplementary Table S4. Heatmaps were generated using Cluster and Tree View (28). *P*-values for protein expression differences between groups were determined in BRB-ArrayTools using a random variance model.

Immunohistochemical Staining

FFPE tissue blocks were cut into 5-μm sections, which were stained with BRAF_V600E (1:50, Spring Bioscience E1929), RB_pS807_S811 (1:50, Cell Signaling Technology 8516), and GSK3α/β_pS21/S9 (1:50, Cell Signaling Technology 9331) antibodies. Stained slides were reviewed by a pathologist (AJL, MTT, or VP) to determine the percentage of positively stained cells among all tumor cells and the average intensity of staining. The intensity of staining for each slide was assigned a score of 0 to 3 (0=negative, 1=low,

Conflict of interest: K.A. and D.S. are employees of Novartis. M.A.D. has served on advisory committees for GlaxoSmithKline, Genentech, and Novartis, and has received research support from GlaxoSmithKline, Genentech, Merck, AstraZeneca, Oncothyreon, and Myriad.

2=intermediate, and 3=strong). Slides with insufficient viable tumor tissues were excluded from analyses.

Results

Hotspot Mutation Analysis

Sufficient DNA was available from matching resected brain and extracranial metastases from 16 patients to undergo Sequenom mass-array analysis for a panel of 154 recurrent hotspot mutations previously reported in cancer (Supplementary Tables S2 and S3). For two samples with low-confidence *BRAF* V600E calls, the presence of mutant BRAF V600E protein was validated by immunohistochemical (IHC) assay. Sequenom and BRAF V600E IHC analyses of the brain metastases detected *BRAF* V600 mutations in seven (44%) and *NRAS* Q61 mutations in three (19%) patients. *CTNNB1* S45 mutations were found in two brain metastases (13%), one of which contained a concurrent *NRAS* Q61 mutation (Table 1). Brain metastases and matched extracranial metastases were 100% concordant for *BRAF* mutation status among the 16 pairs. For *NRAS*, a Q61H mutation call for one sample (extracranial metastasis of patient 17) was indeterminate because the mutation was detected in only one of the two technical replicates; all other paired samples were concordant. *CTNNB1* S45 mutations were 100% concordant among the 16 pairs of matched metastases. These results suggest identical patterns of the recurrent hotspot oncogenic mutations tested in melanoma brain and extracranial metastases in individual patients.

Copy Number Variation Landscape

CNVs were identified in matched tumors using molecular inversion probe (MIP) arrays. After quality control analysis, CNV profiles were obtained from 10 pairs of matched brain and extracranial metastases. Frequent (>35%) gains of large chromosomal regions in 1q, 6p, 7p, 7q, 8q, and 17q and losses in 6q, 8p, 9p, 9q, 10p, and 10q were observed in the brain metastases compared to normal germline DNA (Fig. 1A). The same CNVs were detected at similar frequencies in the matched extracranial metastases (Fig. 1A). Of note, CNVs in these regions have previously been reported in melanoma (29, 30). To compare CNV profiles between individual pairs of tumors, unsupervised hierarchical clustering was performed using the copy number (CN) data for the 20 matching samples. In the resulting dendrogram, the 10 brain metastases did not cluster together, indicating no broad similarity in CNV profiles among brain metastases (Fig. 1B). While five of 10 (50%) brain metastases clustered with the respective matched extracranial metastases (patients 03, 04, 05, 09, and 13), CNV profiles were substantially different between matched tumors in some patients (e.g., patients 12 and 15).

We then compared the frequencies of CNVs between matched brain (N=10) and extracranial (N=10) metastases to identify genes with significant CN differences. Forty-one genes on chromosomes 13 and 15 were found with significant CN difference (P<0.05) between brain and extracranial metastases (Supplementary Table S5). However, in an independent cohort of 20 unmatched melanoma metastases, none of the 41 genes were significantly different in CN between brain (N=10) and extracranial (N=10) metastases.

CNVs were analyzed for oncogenes and tumor suppressors previously reported to be affected by focal amplifications (BRAF, CDK4, CCND1, AKT3, MDM2, MDM4, KIT, MITF, TBX2, MYC, and *TERT*) or deletions (*CDKN2A* and *PTEN*) in melanoma (29, 31-33) in the matched cohort of 10 brain and 10 extracranial metastases (Supplementary Table S6 and Fig. 1C). The results showed that CNV frequencies in these 13 genes were similar between matched brain and extracranial metastases (Fig. 1C), although CNVs between matched samples were often discordant in some genes (e.g., *MITF*, Supplementary Table S6).

Gene Expression Profiling

Whole-genome mRNA gene expression profiling was performed on mRNA from frozen tissue samples for 27 brain metastases and 25 extracranial metastases, including six pairs of matched samples. All patient-matched samples (N=12, Supplementary Table S2) clustered with each other in hierarchical clustering of gene expression data (Fig. 2A and Supplementary Fig. S1), suggesting highly concordant gene expression patterns overall between matching brain and extracranial metastases from individual patients.

Melanoma-related genes analyzed for CNVs (Fig. 1C) were analyzed for significant differences in mRNA expression levels between the patient-matched pairs of brain and extracranial metastases (Fig. 2B). This analysis identified no significant (P<0.05) differences in the expression of BRAF, CDK4, CCND1, AKT3, MDM2, MDM4, KIT, MITF, MYC, TERT, or *PTEN* between the paired samples. *TBX2* showed a trend for increased expression in brain metastases (P=0.10, median ratio brain/extracranial=1.4), while *CDKN2A* expression was significantly lower in brain metastases (P=0.009, median ratio brain/extracranial=0.8). Although CN analysis identified fewer *PTEN* copies in the brain metastases of two patients (03 and 10) (Supplementary Table S6), patient 03 was the only patient with available gene expression data. In this patient *PTEN* expression in the extracranial metastasis was much higher than in the brain metastasis (Supplementary Fig. S2).

Paired *t*-testing of matched brain and extracranial metastases identified 86 genes with significant differences in expression (P<0.01 and fold change of mean expression >1.5, Supplementary Table S7). There was no overlap between the 86 genes and the 41 genes that demonstrated at least one-copy change between matched brain and extracranial metastases (Supplementary Table S5). Analysis of the 86 genes in the unmatched brain (N=21) and extracranial (N=19) metastases showed that three genes also demonstrated significant (P<0.05) differences in expression in this independent cohort of patients: *SGK3, SGSM2* and *ELOVL2*. All three genes were overexpressed in the brain metastases in both the matched (Fig. 2C) and unmatched (Fig. 2D) sample sets. The significant differences in the matched samples were confirmed by quantitative RT-PCR (Supplementary Fig. S3).

Protein Expression Profiling by Reverse Phase Protein Array

Reverse-phase protein array analysis (RPPA) was performed on protein lysates extracted from frozen tumor tissue to quantitatively measure the expression levels of total- and phospho-proteins (Supplementary Table S4). After quality control analysis, expression data

for 152 proteins were available for nine brain and 20 extracranial metastases, which included seven matched pairs of samples. Unsupervised hierarchical clustering of the data for all 152 proteins for the full cohort of samples (N=29) found that six of the seven brain metastases clustered with matching extracranial metastasis from the same patient (Fig. 3A). Thus, overall similar patterns of protein expression were seen in paired samples from individual patients.

Paired t-testing of the seven pairs of matched tumors identified two proteins with significantly different expression between brain and extracranial metastases (P<0.05 and fold change >1.5), both of which were overexpressed in the brain metastases: AKT_pS473 (P=0.0078, average fold change =2.0) and RB_pS807_S811 (P=0.0011, average fold change =1.8). AKT_pS473 expression was more than two-fold higher in the brain metastasis in five of seven paired samples (Fig. 3B), and RB_pS807_S811 was higher in the brain metastasis in all seven pairs (Supplementary Fig. S4). Three other activation-specific markers in the PI3K/AKT pathway also showed evidence of increased expression in matched brain metastases: GSK3β_pS9 (P=0.03, average fold change =1.4), GSK3α/β_pS21/S9 (P=0.16, average fold change =1.3), and PRAS40_ pT246 (P=0.18, average fold change =1.1). In contrast, PTEN protein levels were largely equivalent between matched brain and extracranial metastases (Fig. 3C). Notably, in patient 03 the brain metastasis demonstrated copy loss of *PTEN* and reduced *PTEN* mRNA compared to the extracranial metastasis, but the PTEN protein expression was similar between the matched tumors.

In the unsupervised clustering analysis of all proteins assessed by RPPA, AKT_pT308, AKT_pS473, GSK3β _pS9, GSK3α/β_pS21/S9, and PRAS40_pT246 were tightly clustered ("PI3K/AKT pathway" in Fig. 3A), and thus likely together represent the PI3K/AKT pathway activation signature. Unsupervised clustering of the full cohort of 29 samples by the expression of these five phospho proteins showed that eight of the nine brain metastases (89%) exhibited increased activation of the PI3K/AKT pathway, which was significantly more frequent than was observed in the extracranial metastases (six of 20, 30%, P=0.0052 by Fisher's exact test) (Fig. 3D).

Immunohistochemistry

Immunohistochemistry (IHC) assay was used to evaluate key findings from the high-throughput analyses in a larger set of matched tumors, and to confirm that detected differences were observed in tumor cells. PTEN expression by IHC was scored as Absent (<10% of cells with staining equivalent to internal positive controls, Supplementary Fig. S5) or Present (≥10%) based on a previous analysis that showed that complete loss of PTEN correlated with increased expression of P-AKT (34). Overall, PTEN IHC was performed on 20 pairs of matched brain and extracranial metastases. The results showed that 5% of patients had brain metastasis-only PTEN loss, while 10% of patients had extracranial metastasis-only PTEN loss (Fig. 4A).

As a previous report had already evaluated P-AKT IHC in matched brain and extracranial metastases (20), and RPPA analysis demonstrated that two different antibodies detected significantly increased phosphorylation of the AKT-substrate GSK3 in brain metastases, the expression of GSK3α/β_pS21/S9 was evaluated by IHC. Analysis of the intensity of

GSK3α/β_pS21/S9 staining in 26 pairs of samples confirmed higher expression in melanoma brain metastases than in the matching extracranial metastases ($P<0.05$ by paired *t*-test, Supplementary Fig. S6). GSK3α/β_pS21/S9 expression was higher in the brain metastasis in 69.2% of paired samples, with 19.2% exhibiting >4-fold increase (Fig. 4B). As an example of marked increase in GSK3α/β_pS21/S9 in brain metastasis, images of the brain and extracranial metastases from patient 57 are shown in Fig. 4C.

IHC for RB_pS807_S811 was performed in 25 pairs of matched brain and extracranial metastases. In most samples, only a small percentage of tumor cells were positive for RB_pS807_S811 staining, as in EM_02 (Supplementary Fig. S7A), but a higher percentage of RB_pS807_S811-positive cells were also found in some samples, such as BM_02 (Supplementary Fig. S7A). While there was a slight increase in percentage of cells positively stained for RB_pS807_S811 in the brain metastases, overall there was no significant difference in the IHC staining of tumor cells in the extended cohort of matched brain and extracranial metastases ($P=0.50$ in paired *t*-test; Supplementary Fig. S7B and S7C).

Discussion

More effective therapies for patients with brain metastases must be developed to improve long-term treatment outcomes and survival in patients with metastatic melanoma. In order to improve our understanding of the molecular basis of these tumors, and to develop rational therapeutic approaches for them, we have systematically characterized patient-matched melanoma brain and extracranial metastases for recurrent oncogenic mutations, CNVs, patterns of gene expression, and protein expression and activation. Our results show that despite the overall similarity of the patient-matched brain and extracranial metastases, brain metastases demonstrate specific molecular differences in the PI3K/AKT pathway. These findings add to the growing literature supporting the presence of brain metastasis-specific molecular aberrations in cancer. In addition, they suggest that inhibition of the PI3K/AKT pathway may be a rational therapeutic strategy for patients with melanoma brain metastases.

MAPK pathway inhibitors (i.e., vemurafenib, dabrafenib, trametinib) have demonstrated remarkable clinical activity in patients with metastatic melanoma and have recently gained regulatory approval (35). However, multiple lines of evidence support that the PI3K/AKT pathway may also be an important therapeutic target in this disease, particularly as a combinatorial strategy (36). PTEN loss of function has been detected in 10-30% of melanomas, most frequently in tumors with concurrent activating *BRAF* mutations. Activating mutations in *AKT1* and *AKT3* have been identified as rare events (1-2%) in melanoma, and to date have all been found in tumors with concurrent *BRAF* mutations. Results from whole-exome sequencing confirmed the frequent loss of PTEN function through mutation or copy loss in treatment-naïve melanomas, particularly in tumors with activating *BRAF* mutations (32, 37). Whole exome sequencing also identified *RICTOR* (rapamycin-insensitive companion of mTOR) copy number gain in *BRAF*/*NRAS*-wild-type melanomas, suggesting that these tumors may have elevated PI3K/AKT/mTOR (mammalian target of rapamycin) signaling (37). Whole exome sequencing of tumors collected after progression on selective BRAF inhibitors also identified somatic alterations predicted to

activate the PI3K/AKT pathway that were not detected in pre-treatment samples from the same patients in 22% of the samples, thus also implicating the pathway in acquired resistance (38). Activation of the PI3K/AKT pathway via compensatory signaling through receptor tyrosine kinases (RTKs) has also been observed to correlate with *de novo* and acquired resistance in *BRAF*-mutant cell lines and clinical samples treated with BRAF or MEK inhibitors (28, 39, 40). Notably, upregulation of RTK signaling can be mediated by epigenetic or tumor microenvironment-driven mechanisms (41, 42). The finding that PI3K/AKT activation mediates BRAF inhibitor resistance further supports the rationale for clinical testing of combined inhibition of both MAPK and PI3K/AKT pathways in melanoma.

Previously we identified significantly higher expression of multiple activation-specific markers in the PI3K/AKT pathway in the brain metastases (N=10) than in the liver (N=5) or lung (N=5) metastases in a pilot study using RPPA(17). The lack of paired metastases in that study made it unclear whether this result was brain metastasis specific, or reflected a generalized phenotype of patients who develop brain metastases. Studies are ongoing to assess the power of PI3K/AKT pathway activation to predict risk of brain metastasis development, and the results of our current study do not preclude a positive correlation. However, the proteomic analysis of the cohort of matching brain and extracranial metastases from patients with both tumor types included in the study presented here supports that activation of the PI3K/AKT pathway is particularly enriched in brain metastases. This finding is consistent with a recent report by Niessner *et al.* in which IHC for AKT_pT308 found higher expression in the brain metastases in eight of nine patients with matched brain and extracranial metastases (20). Our study provides both an independent validation of that finding, and additional supporting evidence through the assessment of other pathway activation markers, along with confirmatory IHC for GSK3α/β _pS21/S9.

The mechanism causing increased PI3K/AKT activation in patient-matched melanoma brain metastases remains unclear at this time. We did not observe brain metastasis-only mutations or copy number gain of *PIK3CA* or *AKT* in any of the matched samples. Two of the 10 (20%) paired samples did show fewer copies in the *PTEN* region in the brain metastases. However, neither RPPA nor IHC analysis identified overall decreased PTEN protein expression in brain metastases comparing to matched extracranial metastases. While it did not include analysis of CNV or mRNA, the IHC-based analysis by Niessner *et al.* detected brain metastasis-only PTEN loss in three of nine patients, consistent with the finding that differential PTEN loss is present in only a subset of patients with evidence of increased P-AKT (20). As our study did not include whole-exome analysis of mutational events, we cannot exclude the possibility that other mutations or CNVs could be present in the brain metastases that result in increased PI3K/AKT pathway activation. Such analyses will be performed in the future. However, an alternative hypothesis is that the activation of the PI3K/AKT pathway could be due, at least in part, to interactions between the tumor cells and the tumor microenvironment in the brain. Previously published preclinical experiments showed that the brain TME may induce significant changes in gene expression in melanoma cells (43). In addition, astrocyte-conditioned media strongly increased P-AKT and invasiveness in melanoma cells, while fibroblast-conditioned media had minimal effect in a separate study (20). These results support that the observed increased activation of

PI3K/AKT in brain metastases could be induced by extrinsic factors in the brain microenvironment instead of by intrinsic factors in the tumor cells.

The observed activation of the PI3K/AKT pathway in brain metastases suggests this pathway as a therapeutic target. In a pilot study, we observed that treatment with the PI3K inhibitor BKM120 improve the survival of mice bearing intracranial tumors of the *BRAF* mutant, PTEN-intact human melanoma cell line A375 in a dose-dependent manner (Supplementary Fig. S8A). Combined treatment with BKM120 and the BRAF inhibitor LGX818 also improved survival compared to treatment with LGX818 alone (Supplementary Fig. S8B). However, Western blotting of untreated tumors showed that the levels of AKT_pS473 were not increased in A375 brain metastases as compared to subcutaneous tumors, in contrast to the consistent increase observed in patients (Supplementary Fig. S9). Thus, although the observed effects are promising, additional melanoma cell lines and metastatic sites are currently being evaluated to determine if models can be identified that recapitulate the differences observed in patients for further therapeutic testing.

In conclusion, our study represents to our knowledge the first concurrent profiling of DNA hotspot mutations, DNA copy number variations, mRNA expression patterns, and protein network activation in clinical samples of patient-matched brain and extracranial metastases of any tumor type. This analysis has found overall similarity in the majority of molecular features of matching melanoma brain and extracranial metastases. However, the results provide additional evidence that increased PI3K/AKT pathway activation is a feature of brain metastases. These results add to our understanding of the status of the PI3K/AKT pathway in melanoma and support the rationale for further testing of this pathway as a therapeutic target in this disease.

Supplementary Material

Refer to Web version on PubMed Central for supplementary material.

Acknowledgments

Financial support: This study was funded by National Cancer Institute grant R01 CA154710. M.A.D. is supported by a Melanoma Research Alliance New Investigator grant, the MD Anderson Physician Scientist Program and the MD Anderson Melanoma Specialized Programs of Research Excellence (SPORE) Young Investigator Award (P50 CA093459) and the Physician-Scientist Award from the Goodfellow Scholar Endowment. Melcore is supported by the MD Anderson SPORE grant P50 CA093459. C.G.P is supported by Sao Paulo Research Foundation – FAPESP/ Brazil – N. 2012/24056-2.

References

1. Hall HI, Miller DR, Rogers JD, Bewerse B. Update on the incidence and mortality from melanoma in the United States. J Am Acad Dermatol. 1999; 40:35–42. [PubMed: 9922010]
2. Jemal A, Saraiya M, Patel P, Cherala SS, Barnholtz-Sloan J, Kim J, et al. Recent trends in cutaneous melanoma incidence and death rates in the United States, 1992-2006. J Am Acad Dermatol. 2011; 65:S17–25. e1–3. [PubMed: 22018063]
3. Sawaya, R.; Bindal, RK.; Lang, FF.; Abi-Said, D. Metastatic brain tumors. In: Kaye, AH.; Laws, ERJ., editors. Brain Tumors. 2nd ed.. Churchill Livingstone; Philadelphia: 2001. p. 999-1026.

4. Lotze, MT.; Dallal, RM.; Kirkwood, JM.; Flickinger, JC. Cutaneous melanoma. In: DeVita, VT.; Hellman, S.; Rosenberg, SA., editors. Cancer: Principles and Practice of Oncology. 6th ed.. Lippincott Wiliams and Wilkins; Philadelphia: 2001. p. 2012-69.
5. Kim KB, Flaherty KT, Chapman PB, Sosman JA, Ribas A, McArthur GA, et al. Pattern and outcome of disease progression in phase I study of vemurafenib in patients with metastatic melanoma (MM). ASCO Meeting Abstracts. 2011; 29:8519.
6. Davies MA, Liu P, McIntyre S, Kim KB, Papadopoulos N, Hwu WJ, et al. Prognostic factors for survival in melanoma patients with brain metastases. Cancer. 2011; 117:1687–96. [PubMed: 20960525]
7. Fife KM, Colman MH, Stevens GN, Firth IC, Moon D, Shannon KF, et al. Determinants of outcome in melanoma patients with cerebral metastases. J Clin Oncol. 2004; 22:1293–300. [PubMed: 15051777]
8. Raizer JJ, Hwu WJ, Panageas KS, Wilton A, Baldwin DE, Bailey E, et al. Brain and leptomeningeal metastases from cutaneous melanoma: survival outcomes based on clinical features. Neuro Oncol. 2008; 10:199–207. [PubMed: 18287337]
9. Sampson JH, Carter JH Jr. Friedman AH, Seigler HF. Demographics, prognosis, and therapy in 702 patients with brain metastases from malignant melanoma. J Neurosurg. 1998; 88:11–20. [PubMed: 9420067]
10. Skibber JM, Soong SJ, Austin L, Balch CM, Sawaya RE. Cranial irradiation after surgical excision of brain metastases in melanoma patients. 1996; 3:118–23.
11. Margolin K, Ernstoff MS, Hamid O, Lawrence D, McDermott D, Puzanov I, et al. Ipilimumab in patients with melanoma and brain metastases: an open-label, phase 2 trial. Lancet Oncol. 2012; 13:459–65. [PubMed: 22456429]
12. Long GV, Trefzer U, Davies MA, Kefford RF, Ascierto PA, Chapman PB, et al. Dabrafenib in patients with Val600Glu or Val600Lys BRAF-mutant melanoma metastatic to the brain (BREAK-MB): a multicentre, open-label, phase 2 trial. Lancet Oncol. 2012; 13:1087–95. [PubMed: 23051966]
13. Bos PD, Zhang XH, Nadal C, Shu W, Gomis RR, Nguyen DX, et al. Genes that mediate breast cancer metastasis to the brain. Nature. 2009; 459:1005–9. [PubMed: 19421193]
14. Gomez-Roca C, Raynaud CM, Penault-Llorca F, Mercier O, Commo F, Morat L, et al. Differential expression of biomarkers in primary non-small cell lung cancer and metastatic sites. J Thorac Oncol. 2009; 4:1212–20. [PubMed: 19687761]
15. Milas I, Komaki R, Hachiya T, Bubb RS, Ro JY, Langford L, et al. Epidermal growth factor receptor, cyclooxygenase-2, and BAX expression in the primary non-small cell lung cancer and brain metastases. Clin Cancer Res. 2003; 9:1070–6. [PubMed: 12631609]
16. Sun M, Behrens C, Feng L, Ozburn N, Tang X, Yin G, et al. HER family receptor abnormalities in lung cancer brain metastases and corresponding primary tumors. Clin Cancer Res. 2009; 15:4829–37. [PubMed: 19622585]
17. Davies MA, Stemke-Hale K, Lin E, Tellez C, Deng W, Gopal YN, et al. Integrated Molecular and Clinical Analysis of AKT Activation in Metastatic Melanoma. Clin Cancer Res. 2009; 15:7538–46. [PubMed: 19996208]
18. Huang FJ, Steeg PS, Price JE, Chiu WT, Chou PC, Xie K, et al. Molecular basis for the critical role of suppressor of cytokine signaling-1 in melanoma brain metastasis. Cancer Res. 2008; 68:9634–42. [PubMed: 19047140]
19. Xie TX, Huang FJ, Aldape KD, Kang SH, Liu M, Gershenwald JE, et al. Activation of stat3 in human melanoma promotes brain metastasis. Cancer Res. 2006; 66:3188–96. [PubMed: 16540670]
20. Niessner H, Forschner A, Klumpp B, Honegger JB, Witte M, Bornemann A, et al. Targeting hyperactivation of the AKT survival pathway to overcome therapy resistance of melanoma brain metastases. Cancer Medicine. 2013; 2:76–85. [PubMed: 24133630]
21. Hamilton R, Krauze M, Romkes M, Omolo B, Konstantinopoulos P, Reinhart T, et al. Pathologic and gene expression features of metastatic melanomas to the brain. Cancer. 2013; 119:2737–46. [PubMed: 23695963]

22. Comprehensive molecular portraits of human breast tumours. Nature. 2012; 490:61–70. [PubMed: 23000897]
23. Tibes R, Qiu Y, Lu Y, Hennessy B, Andreeff M, Mills GB, et al. Reverse phase protein array: validation of a novel proteomic technology and utility for analysis of primary leukemia specimens and hematopoietic stem cells. Mol Cancer Ther. 2006; 5:2512–21. [PubMed: 17041095]
24. Davies MA, Stemke-Hale K, Tellez C, Calderone TL, Deng W, Prieto VG, et al. A novel AKT3 mutation in melanoma tumours and cell lines. Br J Cancer. 2008; 99:1265–8. [PubMed: 18813315]
25. Wang Y, Carlton VE, Karlin-Neumann G, Sapolsky R, Zhang L, Moorhead M, et al. High quality copy number and genotype data from FFPE samples using Molecular Inversion Probe (MIP) microarrays. BMC Med Genomics. 2009; 2:8. [PubMed: 19228381]
26. Simon R, Lam A, Li MC, Ngan M, Menenzes S, Zhao Y. Analysis of gene expression data using BRB-ArrayTools. Cancer Inform. 2007; 3:11–7. [PubMed: 19455231]
27. Wright GW, Simon RM. A random variance model for detection of differential gene expression in small microarray experiments. Bioinformatics. 2003; 19:2448–55. [PubMed: 14668230]
28. Gopal YN, Deng W, Woodman SE, Komurov K, Ram P, Smith PD, et al. Basal and treatment-induced activation of AKT mediates resistance to cell death by AZD6244 (ARRY-142886) in Braf-mutant human cutaneous melanoma cells. Cancer Res. 2010; 70:8736–47. [PubMed: 20959481]
29. Jonsson G, Dahl C, Staaf J, Sandberg T, Bendahl PO, Ringner M, et al. Genomic profiling of malignant melanoma using tiling-resolution arrayCGH. Oncogene. 2007; 26:4738–48. [PubMed: 17260012]
30. Kabbarah O, Nogueira C, Feng B, Nazarian RM, Bosenberg M, Wu M, et al. Integrative genome comparison of primary and metastatic melanomas. PLoS One. 2010; 5:e10770. [PubMed: 20520718]
31. Gembarska A, Luciani F, Fedele C, Russell EA, Dewaele M, Villar S, et al. MDM4 is a key therapeutic target in cutaneous melanoma. Nat Med. 2012; 18:1239–47. [PubMed: 22820643]
32. Hodis E, Watson IR, Kryukov GV, Arold ST, Imielinski M, Theurillat JP, et al. A landscape of driver mutations in melanoma. Cell. 2012; 150:251–63. [PubMed: 22817889]
33. Kraehn GM, Utikal J, Udart M, Greulich KM, Bezold G, Kaskel P, et al. Extra c-myc oncogene copies in high risk cutaneous malignant melanoma and melanoma metastases. Br J Cancer. 2001; 84:72–9. [PubMed: 11139316]
34. Davies MA, Chen G, Liu DD, Malke J, Gershenwald JE, Lazar AJ. Abstract 968: Molecular and clinical correlates of PTEN expression in melanoma. Cancer Research. 2012; 72:968.
35. Sullivan RJ, Flaherty K. MAP kinase signaling and inhibition in melanoma. 2013; 32:2373–9.
36. Davies MA. The role of the PI3K-AKT pathway in melanoma. Cancer J. 2012; 18:142–7. [PubMed: 22453015]
37. Krauthammer M, Kong Y, Ha BH, Evans P, Bacchiocchi A, McCusker JP, et al. Exome sequencing identifies recurrent somatic RAC1 mutations in melanoma. Nat Genet. 2012; 44:1006–14. [PubMed: 22842228]
38. Shi H, Hugo W, Kong X, Hong A, Koya RC, Moriceau G, et al. Acquired resistance and clonal evolution in melanoma during BRAF inhibitor therapy. Cancer Discov. 2014; 4:80–93. [PubMed: 24265155]
39. Nazarian R, Shi H, Wang Q, Kong X, Koya RC, Lee H, et al. Melanomas acquire resistance to B-RAF(V600E) inhibition by RTK or N-RAS upregulation. Nature. 2010; 468:973–7. [PubMed: 21107323]
40. Villanueva J, Vultur A, Lee JT, Somasundaram R, Fukunaga-Kalabis M, Cipolla AK, et al. Acquired resistance to BRAF inhibitors mediated by a RAF kinase switch in melanoma can be overcome by cotargeting MEK and IGF-1R/PI3K. Cancer Cell. 2010; 18:683–95. [PubMed: 21156289]
41. Abel EV, Basile KJ, Kugel CH 3rd, Witkiewicz AK, Le K, Amaravadi RK, et al. Melanoma adapts to RAF/MEK inhibitors through FOXD3-mediated upregulation of ERBB3. The Journal of clinical investigation. 2013; 123:2155–68. [PubMed: 23543055]

42. Straussman R, Morikawa T, Shee K, Barzily-Rokni M, Qian ZR, Du J, et al. Tumour micro-environment elicits innate resistance to RAF inhibitors through HGF secretion. Nature. 2012; 487:500–4. [PubMed: 22763439]

43. Park ES, Kim SJ, Kim SW, Yoon SL, Leem SH, Kim SB, et al. Cross-species hybridization of microarrays for studying tumor transcriptome of brain metastasis. Proc Natl Acad Sci U S A. 2011; 108:17456–61. [PubMed: 21987811]

Statement of Translational Relevance

While a number of personalized targeted therapies have demonstrated impressive clinical activity, the development of more effective treatments for brain metastases remains a critical challenge. This is particularly true for melanoma, which has a very high rate of brain metastasis. Previous studies have demonstrated that brain metastases can harbor significant molecular differences versus primary tumors. This study represents one of the first multi-modality molecular comparisons of patient-matched brain metastases and extracranial metastases. The high concordance of oncogenic driver mutations is consistent with the clinical activity that has been observed in brain metastases with oncogene-selective targeted therapies (i.e. BRAF inhibitors). However, the discovery of increased activation of the PI3K/AKT pathway in melanoma brain metastases supports the rationale for further evaluation of this pathway as a therapeutic target. The results also support further investigation of metastatic site-specific molecular features.

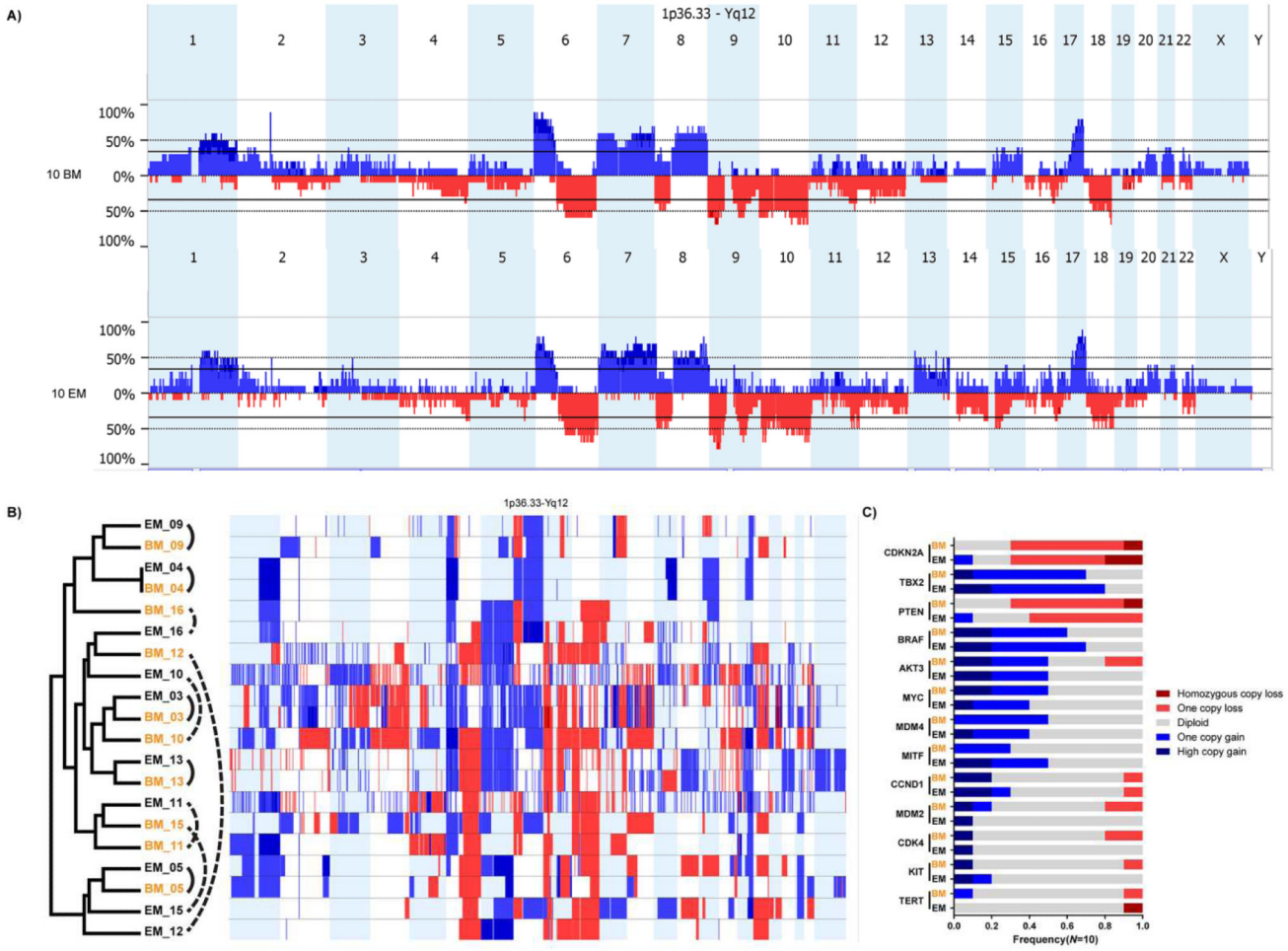

Fig. 1.

Copy number variation (CNV) profiling of brain metastases and extracranial metastases. (**A**) CNV histograms of 10 brain metastases (BM) and the matched 10 extracranial metastases (EM). Frequencies of CN gains (blue, pointing up) and CN losses (red, pointing down) were plotted to their genomic locations. (**B**) Results of unsupervised hierarchical clustering analysis of CNVs in the matched 10 BM and 10 EM. Genome-wide CN gains (light blue=one copy gain, dark blue=high copy gain) and losses (light red=one copy loss, dark red=homozygous copy loss) in each sample are plotted next to the dendrogram. BM are in orange and EM are in black; matched samples are connected by arced lines. Solid lines: matched samples clustering together; dotted lines: matched samples clustering apart. (**C**) CNV frequencies of 13 genes in matched 10 BM (orange) and 10 EM (black). Genes are sorted by the mean CNV frequency in BM and EM, with high on top and low on bottom.

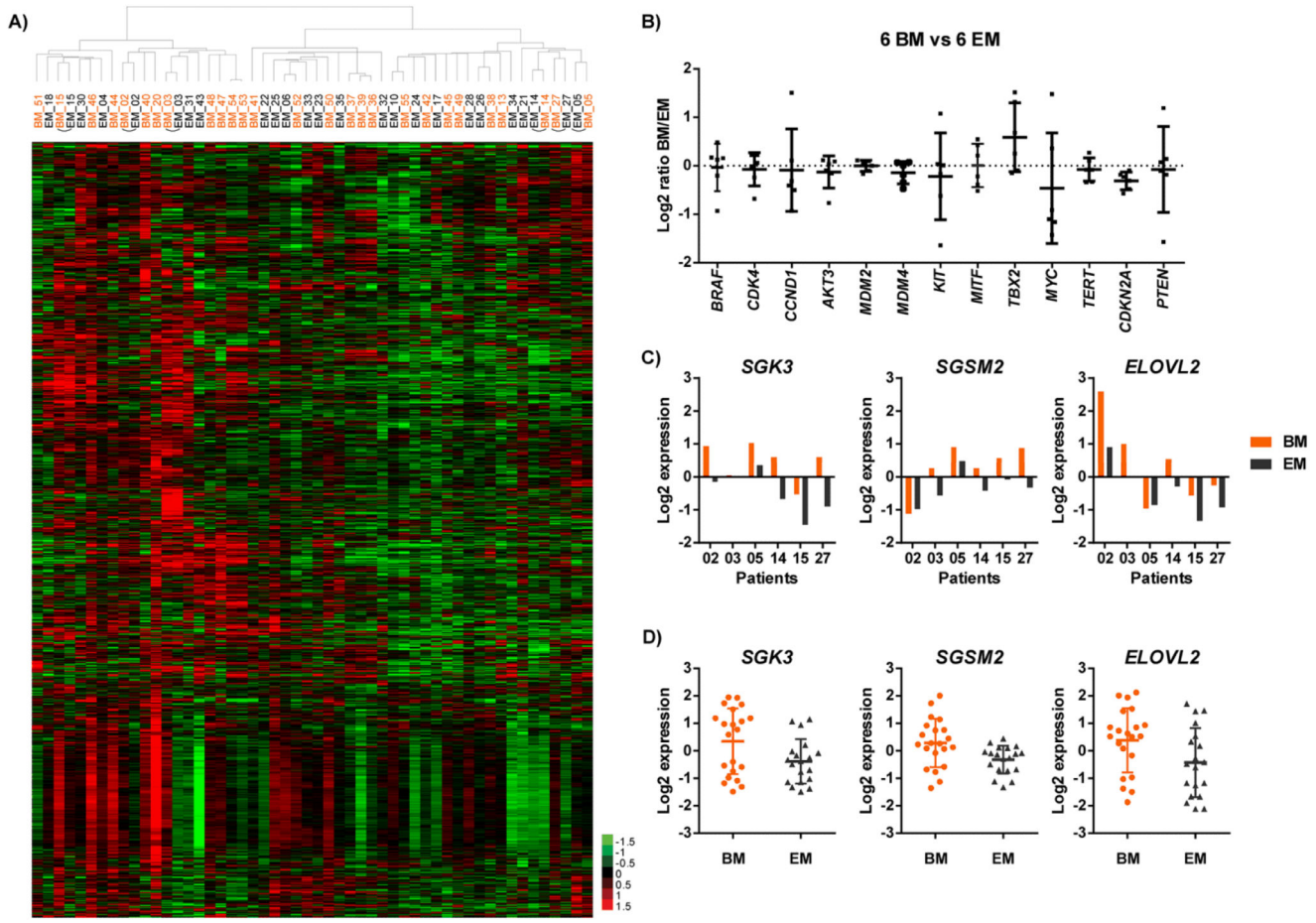

Fig. 2.

Gene expression profiling of brain and extracranial metastases. (**A**) Hierarchical clustering of log2 expression values of 8050 probes in 27 brain metastases (BM, orange) and 25 extracranial metastases (EM, black). Probes that showed less than 1.5-fold change from the median in more than 80% of the samples were excluded. Matched tumors are connected with arcs. (**B**) Differences in expression of 13 genes between paired BM and EM. Fold changes of gene expression from EM to BM were converted into log2 ratios. Log2 ratios in six pairs of samples were plotted as dots for each gene, means and standard deviations were plotted as horizontal bars. (**C**) Expression of *SGK3, SGSM2* and *ELOVL2* in matched BM and EM of six patients. Each column represents the expression value of one sample. (**D**) Expression of *SGK3, SGSM2* and *ELOVL2* in unmatched BM (*N*=21) and EM (*N*=19). Each dot represents the expression value of one sample.

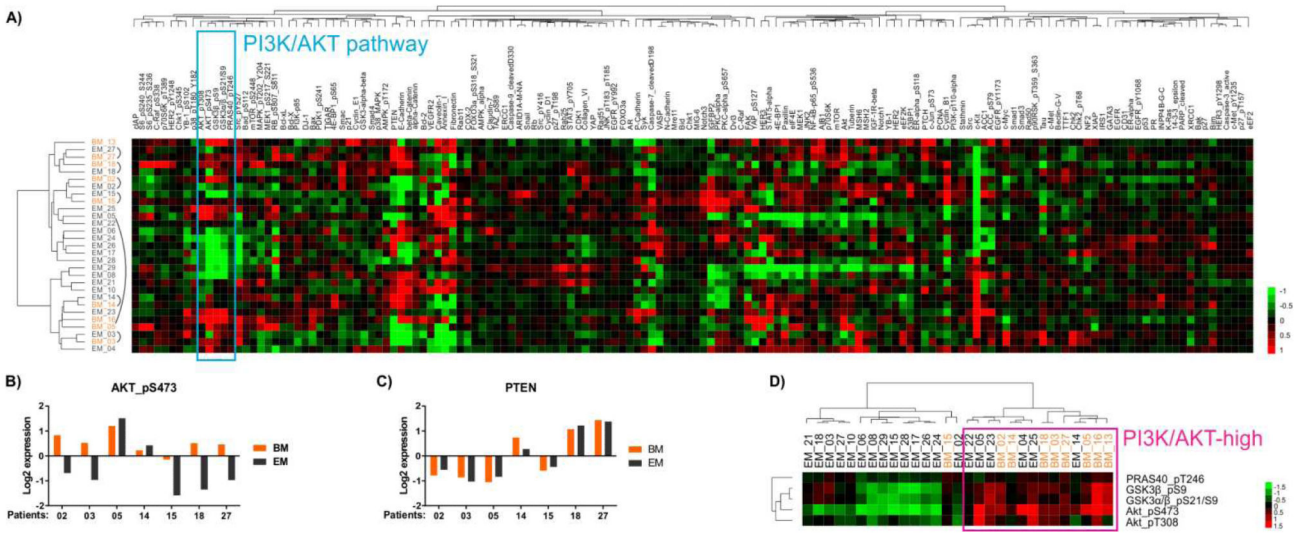

Fig. 3.

Protein expression profiling of brain and extracranial metastases. (**A**) Unsupervised hierarchical clustering of RPPA data from 152 proteins in nine brain metastases (BM, orange) and 20 extracranial metastases (EM, black). Matched tumors are connected by arced lines. The cyan box highlights five phospho proteins of the PI3K/AKT pathway that clustered together. (**B**) Log2 expression levels of AKT_pS473 in seven pairs of matched metastases. Each column represents log2 expression value in one tumor. (**C**) Log2 expression levels of PTEN in seven pairs of matched tumors. (**D**) Unsupervised hierarchical clustering of 29 unmatched tumors using expression data of five phospho proteins highlighted in (**A**), which are activation markers of the PI3K/AKT pathway. The magenta box highlights a cluster of tumors with high PI3K/AKT pathway activity.

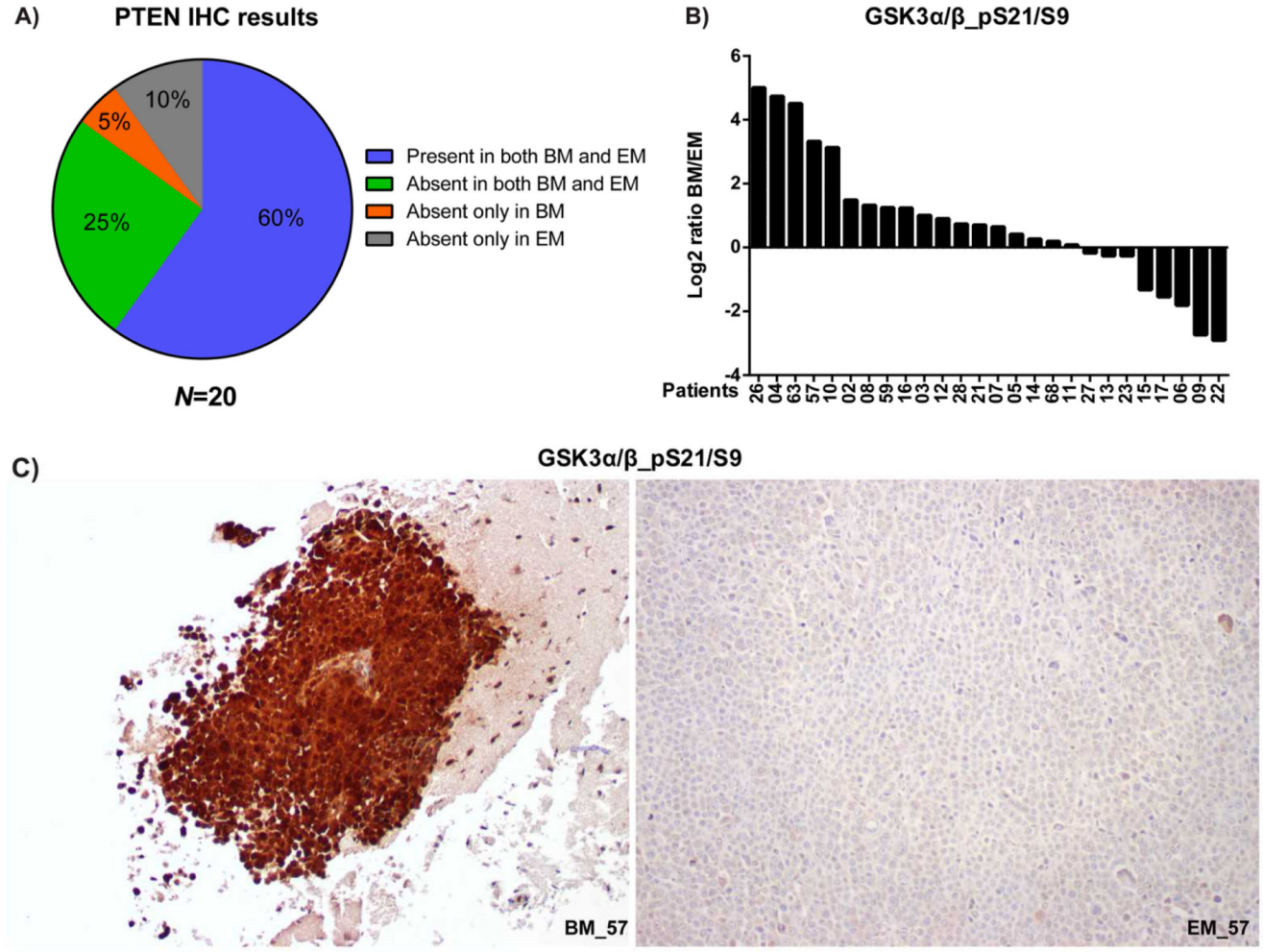

Fig. 4.

Immunohistochemistry (IHC) of PI3K/AKT pathway proteins in matched melanoma metastases. (**A**) PTEN IHC results in 20 pairs of brain metastases (BM) and matched extracranial metastases (EM) were categorized and the incidences displayed. (**B**) Log2 ratio of GSK3α/β_pS21/S9 percentage-adjusted intensity between BM and EM in each of the 26 patients. Patients were sorted from high to low percentage-adjusted intensity. (**C**) Images of GSK3α/β_pS21/S9 IHC in the BM and EM of patient 57. BM_57 was photographed at a lower magnification than EM_57 to show the negative stroma.

Table 1

Mutations in 16 pairs of matched metastases

Patient	Brain metastases	Extracranial metastases
02	*BRAF* V600E	*BRAF* V600E
03	None	None
04	*BRAF* V600E	*BRAF* V600E
05	*BRAF* V600K	*BRAF* V600K
06	*NRAS* Q61K	*NRAS* Q61K
07	*BRAF* V600E	*BRAF* V600E
08	*NRAS* Q61K, *CTNNB1* S45F	*NRAS* Q61K *CTNNB1* S45F
09	None	None
10	CTNNB1 S45P	CTNNB1 S45P
11	*BRAF* V600E	*BRAF* V600E
12	*BRAF* V600E	*BRAF* V600E
13	None	None
14	None	None
15	*BRAF* V600E	*BRAF* V600E
16	None	None
17	*NRAS* Q61H	*NRAS* Q61H*

*One of the two replicate assays called *NRAS* Q61H.